La *et al.*
Journal of Analytical Science and Technology (2023) 14:48
https://doi.org/10.1186/s40543-023-00411-3

Journal of Analytical Science and Technology

RESEARCH ARTICLE

Open Access

Synthesis and evaluation of small molecule-based derivatives as inhibitors of polo-box domain of polo-like kinase-1

Yeo Kyung La[2], Pethaiah Gunasekaran[2], Min Su Yim[1], Gong-Hyeon Lee[2], Yeon Sil Hwang[2], Kannan Damodharan[2], Mi-Hyun Kim[3], Jeong Kyu Bang[1,2,4*] and Eun Kyoung Ryu[1,4*]

Abstract

Objectives Polo-like kinase 1 (Plk1) is an important mitotic protein. In particular, this protein is highly overexpressed in many types of tumors and has been identified as a potential biomarker for the treatment and diagnosis of tumors. Plk1 is composed of two domains, an N-terminal kinase domain and a C-terminal polo-box domain (PBD). Presently, inhibitors with improved selectivity and specificity for Plk1 are unavailable. Therefore, we aimed to develop an inhibitor targeting the C-terminal PBD present only in Plk1.

Methods & results In this study, three derivatives targeting PBD for Plk1 were designed by protein–protein interactions, which showed high levels of selectivity and specificity for Plk1 PBD, and were evaluated to inhibit tumor cell proliferation through an apoptotic process during tumor cell division. The investigation of the in vitro and in vivo antitumor effects of these inhibitors demonstrated that one of the new small molecules, **1**, is a promising anticancer agent.

Conclusion Our findings can provide new insights for the design of novel Plk1 peptide inhibitors in the future.

Keywords Polo-like kinase 1, Polo-box domain, Small molecule, Derivatives, Tumor, Inhibitor

Introduction

Protein–protein interactions (PPI), which occur in the body, are important reactions for understanding the essence of life phenomena and are often present between several proteins in cells. They provide basic and important information on various mutual organic actions such as signal transduction and protein metabolism. Therefore, elucidating PPI and understanding the key binding sites of proteins can reveal biological functions in vivo, leading to the development of new drugs that minimize side effects (Corbi-Verge and Kim 2016; Skwarczynska and Ottmann 2015). Useful information can be obtained from the structures formed when the target protein and the inhibitor bind. In addition, through the analysis of protein-inhibitor interactions, the development and research of selective inhibitors of disease-specific proteins are increasing. Many studies on the development of inhibitors that suppress tumors using the PPI method have been published (Cleary et al. 2014; Tse et al. 2008; Vassilev et al. 2004).

Polo-like kinases (Plks), a subfamily of serine-threonine protein kinases, comprise five classes (Plk1, Plk2, Plk3,

*Correspondence:
Jeong Kyu Bang
bangjk@kbsi.re.kr
Eun Kyoung Ryu
ekryu@kbsi.re.kr
[1] Division of Bioconvergence Analysis, Korea Basic Science Institute, Ochang, Cheongju 28119, Republic of Korea
[2] Dandicure Inc., Ochang, Chungbuk 28119, Republic of Korea
[3] Department of Internal Medicine, Pusan National University School of Medicine and Biomedical Research Institute, Pusan National University Hospital, Busan, Republic of Korea
[4] Korea Basic Science Institute, Ochang, Cheongwon, Chungbuk 363-883, Republic of Korea

Plk4, and Plk5) that play important roles in cell proliferation and division (Archambault and Glover 2009; Park et al. 2010; Strebhardt 2010). Among these, the function of Plk1 is the most well-known. Plk1 plays a role in regulating cytokinesis and cell cycle processes, such as spindle formation, centrosome maturation, mitosis entry, and chromosome separation, and is critically involved in cancer cell proliferation and tumor formation (Luo et al. 2009; Weerdt and Medema 2006; Yun et al. 2009). Unlike normal cells, Plk1 is overexpressed in rapidly proliferating tumor cells and promotes tumor proliferation. Suppression of Plk1 results in apoptosis and M-phase cell cycle arrest in tumor cells (Scharow et al. 2015; Steegmaier et al. 2007). Although the function of Plk1 in the mechanism of tumor proliferation has not been accurately elucidated, Plk1 is an attractive biomarker for researchers. In addition, there is an active trend to develop anticancer drugs that selectively inhibit Plk1 for the effective treatment of various tumors.

Plk1 consists of a kinase domain, an ATP-binding site at the N-terminus, and a polo-box domain (PBD) at the C-terminus, and the development of Plk1 inhibitors is being conducted by targeting two proteins (Lee et al. 2015). Most N-terminal ATP target inhibitors of Plk1 have been developed based on small-molecule compounds. Among them, the most advanced inhibitor for clinical application is the small molecule BI2536, an inhibitor consisting of a dihydropteridinone structure developed by Boehringer Ingelheim. BI2536 targets the kinase domain at the N-terminus of Plk1 and binds to Plk1, inhibiting its activity. BI2536 has high affinity to Plk1 (Plk1: $IC_{50}=0.83$ nM, Plk2: $IC_{50}=3.5$ nM, and Plk3: $IC_{50}=9.0$ nM) (Fode et al. 1994). However, because BI2536 is an inhibitor of the kinase domain (KD), which is an ATP-binding site, it interacts with other nonspecific kinases in vivo, resulting in low selectivity and serious side effects (Karaman et al. 2008).

Therefore, it is necessary to develop inhibitors, targeting PBD, that are more effective than BI2536. To overcome these drawbacks and develop an inhibitor with improved selectivity and specificity for Plk1, we developed small molecule-based derivatives (**1**, **2,** and **3**) targeting the C-terminal PBD present only in Plk1 (Fig. 1).

This study aimed to confirm the anticancer effect of PPIs by developing a PBD structure-based small-molecule inhibitor. The research steps were designed as follows: Firstly, after the PBD structure was identified by the Yun group in 2009 (Yun et al. 2009), we conducted virtual screening of the NIH based on it. Secondly, some of the best candidates were selected and optimized. Thirdly, cell cycle arrest and cancer cell apoptosis were confirmed by inhibitors in vitro. Finally, the in vivo treatment effect of the inhibitor was evaluated using a tumor xenograft mouse model.

Results

Synthesis of 1, 2, and 3

Firstly, N-alkylation of pyrazole aldehyde (**4**) was conducted using N-Boc protected bromoethylamine in the presence of K_2CO_3 in DMF to afford **5** in 70% yield, and Boc group was cleaved using 2 M-HCl in diethylether, providing the corresponding amine hydrochloride (**6**, 96% yield). The compound **6** was treated with 4-(Fmoc-aminomethyl)benzoic acid (**7**) in the presence of EDCI, HOBt, and DIEA in DMF to obtain the amide compound. Condensation with barbituric acid in methanol under reflux conditions yielded **8.** Thereafter, Fmoc group was deprotected using piperidine in DMF to obtain the desired product **1** (53% yield). By adopting similar strategy, 4-(Boc-amino)benzoic acid (**9**) was treated with **6** in the presence of EDCI, HOBt, and DIEA in DMF to afford **10** (59% yield) and refluxed with barbituric acid in methanol, followed by Boc deprotection with TFA, leading to the achievement of the desired product **2** (52% yield). Consequently, 4-(bromomethyl)benzoic acid was chlorinated using $(COCl)_2$ in DMF-DCM solvents to obtain a useful substrate 4-bromomethyl-benzoyl chloride (**11**), which was treated with **6.** Thereafter, nucleophilic substitution reaction with the aid of DIEA in DCM resulted in the corresponding amide derivative **12** (75% yield). Furthermore, the compound **12** refluxed with barbituric acid in methanol gave the condensed component **13** (78% yield). Eventually, the utilization of **13** with N-Boc protected ethylenediamine in DCM and MeOH and deprotection of Boc by TFA assisted reaction led to the successful achievement of the anticipated product **3** (33% yield; Fig. 2).

Human cervical adenocarcinoma epithelial cell line (HeLa) cancer cell viability assay by MTT

As the concentration of **1** increased, the viability of tumor cells decreased, and the IC_{50} value was approximately 272 μM in comparison to that of the control cells (Fig. 3). This result suggests that **1** inhibits the proliferation of HeLa cancer cells by interfering with the Plk1 function.

Delocalization of Plk1 at the kinetochore by small molecule inhibitors

Fluorescent staining indicated the nucleus, kinetochores, and Plk1 as blue, green, and red, respectively (Fig. 4a). DMSO, nocodazole, and **2** and **3** groups showed no change in the position and quantification of Plk1. However, in the groups treated with BI2536 and **1**, the red fluorescence intensity of Plk1 was significantly

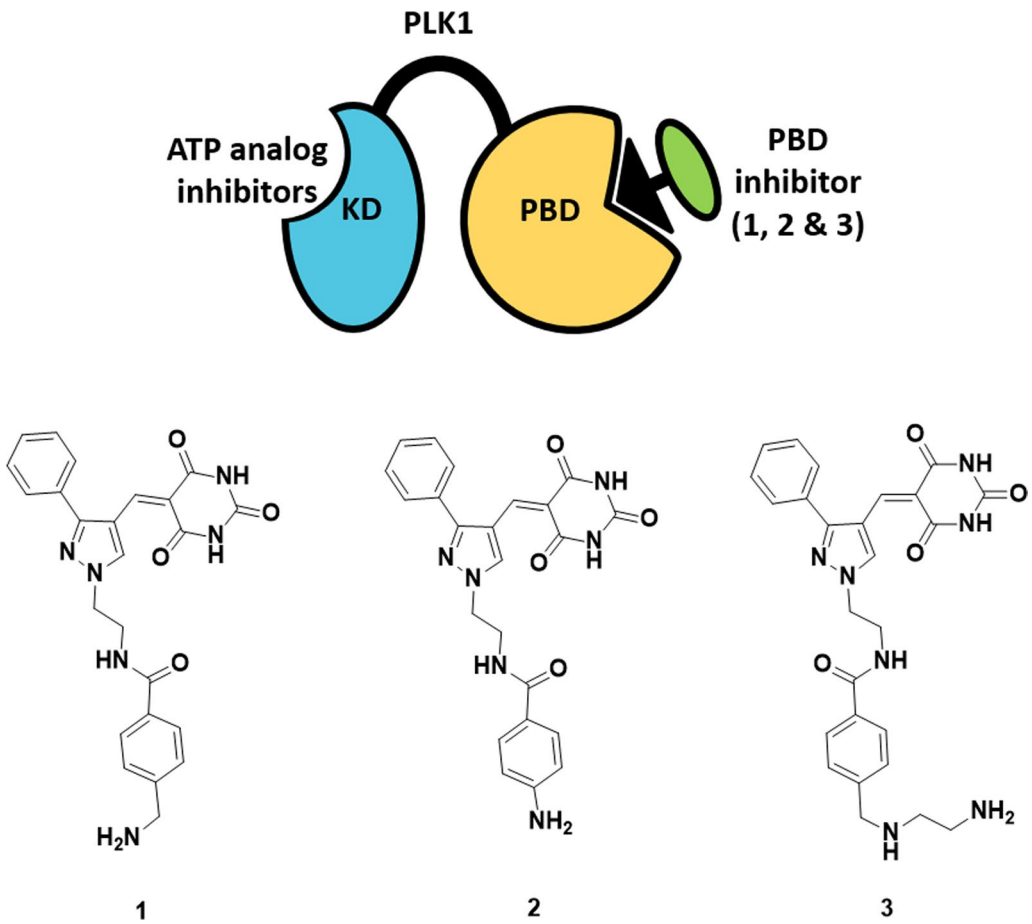

Fig. 1 A schematic diagram illustrating the targeting of Polo-like kinase 1 (Plk1) polo-box domain (PBD) with small molecule-based derivatives, **1**, **2,** and **3**

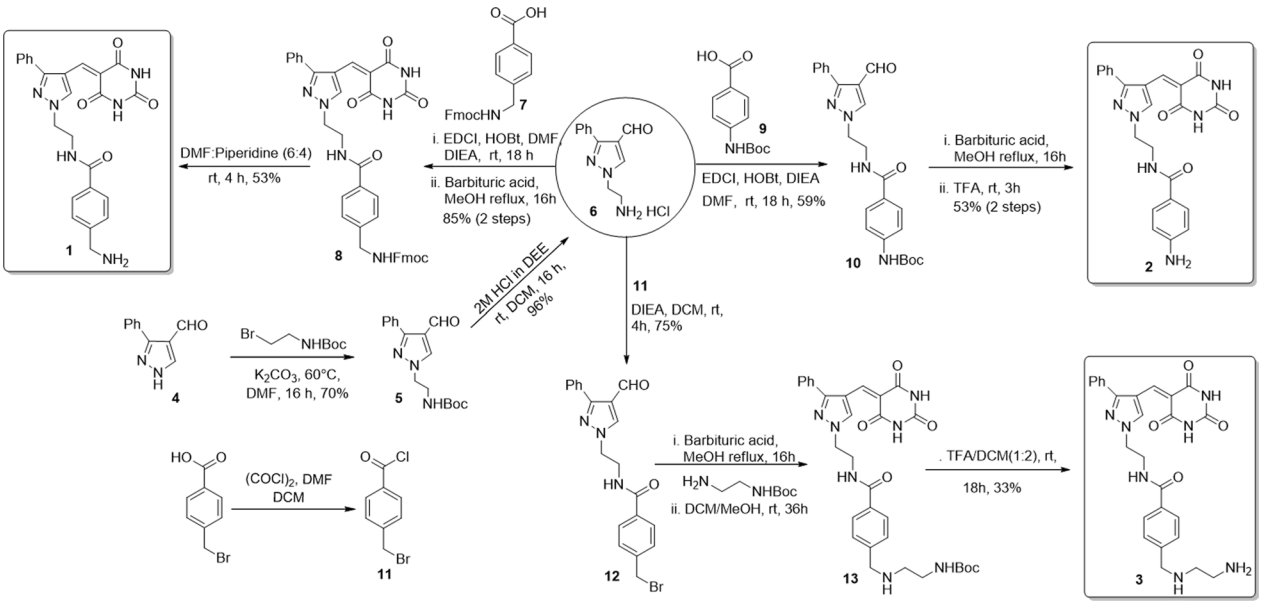

Fig. 2 Synthetic routes for derivatives **1**, **2,** and **3**

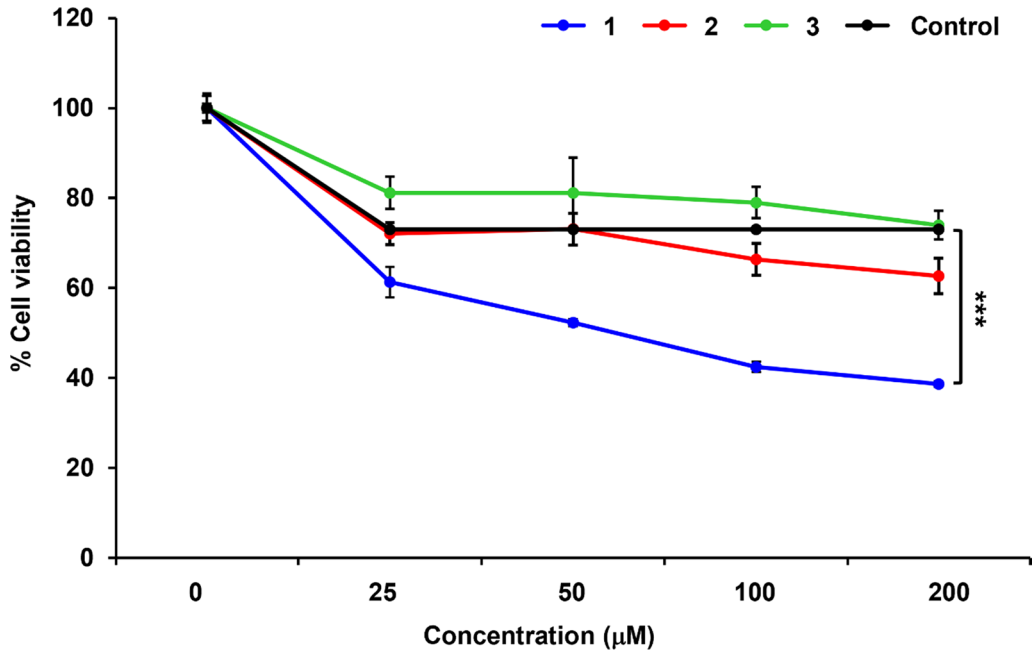

Fig. 3 HeLa cancer cell viability by MTT assay showing a reduction in cell proliferation with different concentrations (0, 25, 50, 100 and 200 μM) of the derivatives, **1**, **2**, and **3** for 24 h. *** $p < 0.001$

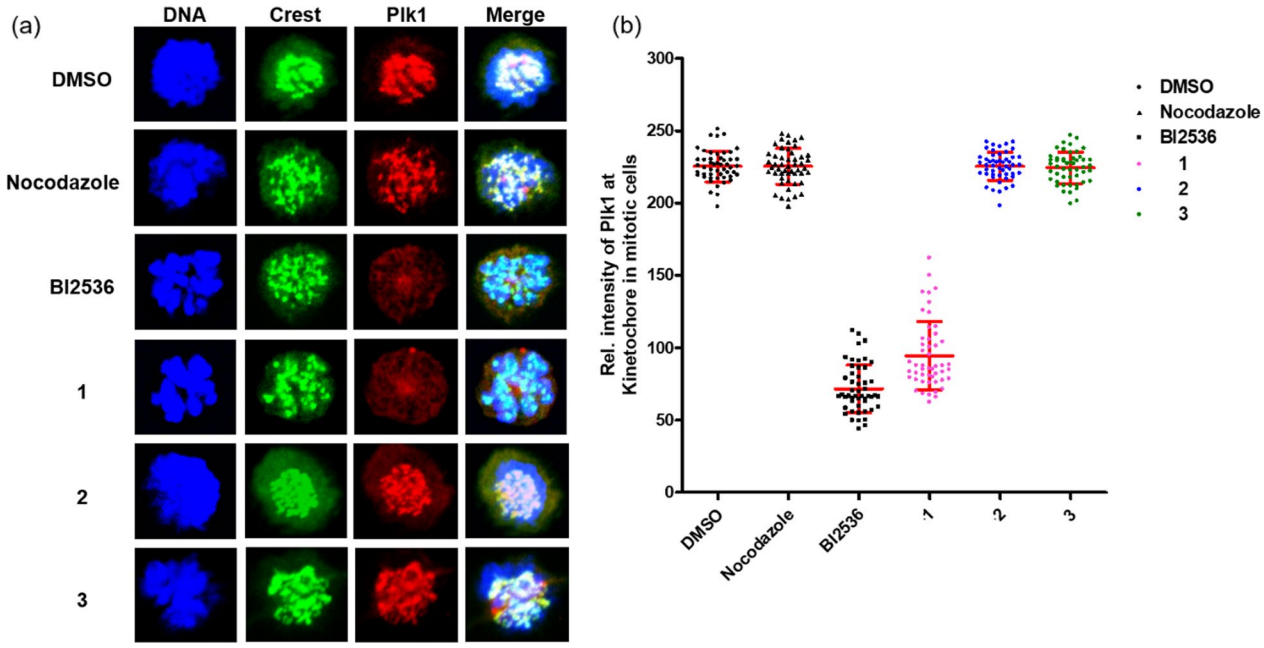

Fig. 4 Plk1 delocalized from the kinetochore of HeLa cells. The cells were treated with DMSO, nocodazole (200 nM), BI2536 (200 nM), and their derivatives (200 μM) for 24 h **a** Representative images show kinetochore (green) and Plk1 (red) fluorescence among prometaphase cells. The phase of the cell was determined by the shape of the DNA (blue). **b** The quantitation graph of Plk1 fluorescence intensity at the kinetochore. The intensity of Plk1 was measured 10 times per cell. "n" represents the cell number

decreased. Plk1 fluorescence intensity of kinetochore decreased by 68.2 and 58.1% for **1** and BI2536, respectively (Fig. 4b).

Cell cycle arrest by small molecule inhibitors via G2/M checkpoint

The groups **2** and **3** showed little change in the G2/M phase compared with the control group. However, the BI2536 and **1** groups induced increase of approximately 10 and 5%, respectively (Fig. 5). These results indicated that, unlike **2** and **3**, only **1** caused cell cycle arrest in cancer cells.

Effect of small molecule inhibitors on cell apoptosis in HeLa cancer cells

Figure 6a shows that BI2536 and **1** induce apoptosis in tumor cells. Captured images are shown in green and red for live and apoptotic cells, respectively. In particular, significant images were obtained at 48 h rather than 24 h. BI2536 showed apoptosis effect of 27.1 ± 4.8% at 24 h and 80.2 ± 5.3% at 48 h, and similarly **1** showed 12.4 ± 4.4% at 24 h and 59 ± 4.9% at 48 h (Fig. 6b). In contrast, **2** and **3** exhibited no apoptotic effects. These results indicated that **1** caused cell cycle arrest in cancer cells and subsequently apoptosis.

In vivo biological effect of small molecule inhibitors for cancer therapy

Compared with the control group, the groups treated with BI2536 and **1** showed a significant decrease in tumor size. The BI2536 treated group showed tumor reductions of 56.6 and 64.6% on 18 and 21 days, respectively. Moreover, group **1** also had significantly decreased tumor size by 47.7 and 45.1 on 18 and 21 days, respectively. The highest in vivo effect of **1** was on the 18th day (Fig. 7a). There was no significant change in the weight (Fig. 7b). As a result, we confirmed that **1** has cancer treatment effects both in vitro and in vivo.

Discussion

Over the past decades, many studies have targeted the kinase domain (KD) of Plk1 to confirm its anticancer effects. BI2536, developed by Boehringer Ingelheim, is a powerful Plk1 inhibitor used in preclinical and clinical trials (Steegmaier et al. 2007). BI2536 has a potent effect (IC_{50} = 0.83 nM), and X-ray co-crystal structure showed that it binds to the KD of Plk1 through hydrogen bonding with R57, L59, and C133 (Kothe et al. 2007). However, BI2536 was terminated in phase II clinical trials because of serious side effects, such as dose-limiting toxicities, neutropenia, and leukopenia (Lund-Andersen et al. 2014; Maire et al. 2013; Yim 2013). Therefore, our group focused on the development of new inhibitors targeting the PBD of Plk1. To develop Plk1 drugs using protein–protein interactions, peptide-based inhibitors have been developed. This is because the interaction area between proteins is wide, and the active site is flat, unlike the ATP pocket. Peptides and peptide mimics have excellent binding abilities. However, their enzyme stability and cell permeability are low. Therefore, much effort is required to develop them into drugs. To overcome these limitations, it is necessary to develop structure-based drug-like small molecules. In this study, small pyrrole-based compounds with different substituents such as -CH_2-NH_2 (**1**), -NH_2 (**2**), and -CH_2-NH-CH_2-CH_2-NH_2 (**3**) were synthesized and evaluated for their anticancer activities. All target derivatives exerted inhibitory effects against HeLa cancer cells that overexpress Plk1. Although similar structures **1**, **2**, and **3** were derived from the basic backbone structure, only **1** was shown to have cancer treatment effects. **1** exhibited significant potency, with an IC_{50} value of 272 μM. Moreover, **1** induced cell cycle arrest and apoptosis after the delocalization of Plk1 in cancer cells in vitro and showed significant cancer treatment effects in vivo. These results are consistent with those of a previous study (Gunasekaran et al. 2020). These promising data will be a good starting point for further design and synthesis of new derivatives as potent and selective PBD inhibitors with antitumoral activity and acceptable properties of drug-like compounds.

Since **1** targets the PBD of Plk1, it is expected to substantially reduce the side effects of BI2536 and BI6727, which target KD. **1** also showed excellent anticancer effects both in vitro and in vivo. In future studies, the solubility of **1** will be improved to identify **1** and PBD binding. Furthermore, structural modifications to improve solubility and cell penetration are required to improve efficacy and various evaluations.

Conclusions

We overcame the limitation of the lack of selectivity and specificity for the target protein, Plk1 PBD, using PPI and investigated the antitumor effect of **1** in vivo as well as in vitro. These results confirmed that the reduction in cancer cell proliferation due to treatment with **1** interfered with the PLK1 of PBD. Our results demonstrate that the new small molecule **1** is a promising anticancer agent. We expect that our study will provide new insights into the design of novel Plk1 inhibitors. Our study has significant implications for the development of anticancer therapies and provides a new scaffold for the development of anticancer drugs using PPIs of Plk1 PBD.

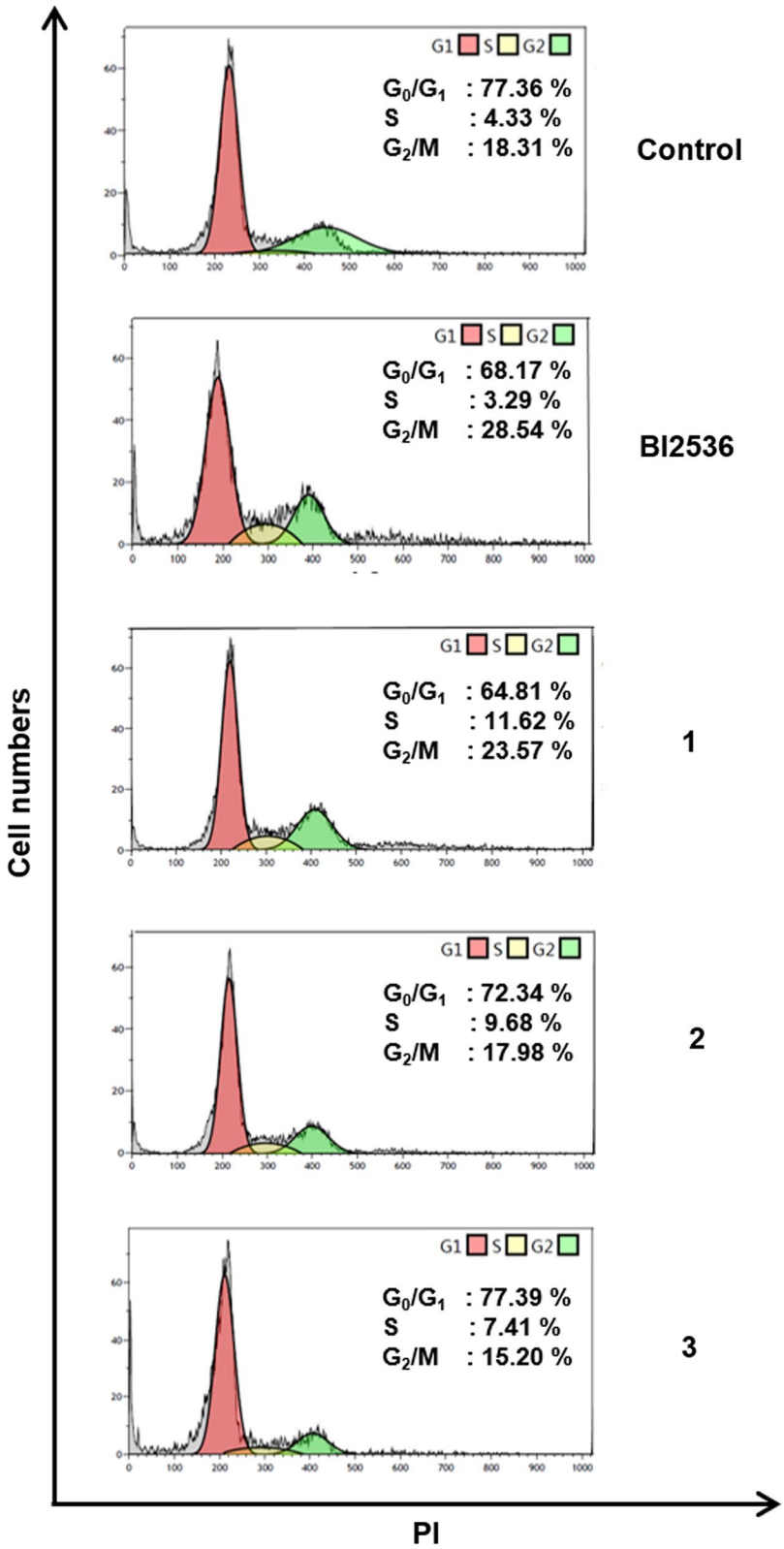

Fig. 5 Analysis of HeLa cells treated with BI2536 (200 nM), **1** (200 μM), **2** (200 μM), and **3** (200 μM) for 18 h using fluorescence-activated cell sorting (FACS)

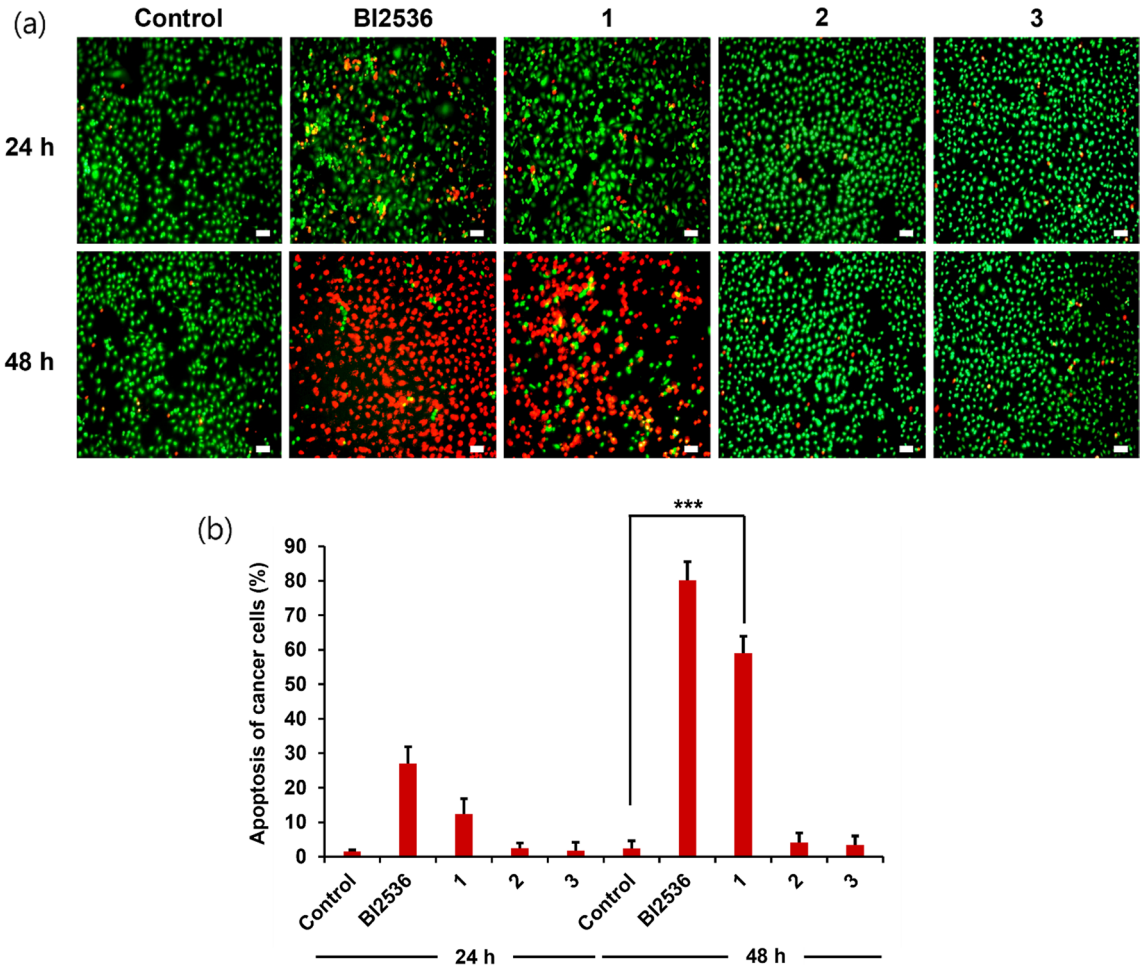

Fig. 6 Fluorescence images of apoptosis using fluorescence microscope (×100 magnification, scale bar: 100 μm). **a** HeLa cells were treated with BI2536 (200 nM) and its derivatives (200 μM) for 24 and 48 h and then stained with fluorescence apoptosis kit. Green and red fluorescence represent live and apoptosis cells, respectively. **b** Apoptosis cells are shown as red bar graphs that represent mean values. ***$p < 0.001$

Methods

Chemistry

tert-butyl (2-(4-formyl-3-phenyl-1H-pyrazol-1-yl)ethyl) carbamate (5)

3-phenyl-1*H*-pyrazole-4-carbaldehyde (**4**) [0.67 g, 0.003912 mol] in anhydrous DMF (5 mL) was added slowly to a stirred solution of 2-(Boc-amino)ethyl bromide (0.795 g, 0.00355 mol) and potassium carbonate (1.47 g, 0.01065 mol) in anhydrous DMF (20 mL). After completion of the addition, the temperature was slowly raised to 60 °C and stirred for 16 h. The reaction was quenched by adding water (30 mL) and extracted with ethyl acetate (30 mL × 3). The combined organic extracts were washed with brine (40 mL), dried over Na_2SO_4, and then evaporated. The crude product was purified via silica gel column chromatography using hexane:ethyl acetate (8:2) mixture to obtain **5** as a white solid (0.687 g, 70%). ^{1}H NMR (500 MHz, $CDCl_3$) δ 9.98 (s, 1H), 8.04 (s, 1H), 7.75 (d, $J = 6.8$ Hz, 2H), 7.56–7.41 (m, 3H), 4.87 (s, 1H), 4.34 (s, 2H), 3.75–3.58 (m, 2H), and 1.47 (s, 9H). ^{13}C NMR (101 MHz, $CDCl_3$) δ 185.2, 154.6, 150.3, 138.4, 134.8, 131.4, 130.1, 129.1, 128.8, 120.9, 120.3, 80.2, 52.4, 40.4, and 28.3.

1-(2-aminoethyl)-3-phenyl-1H-pyrazole-4-carbaldehyde hydrochloride (6)

2 M HCl (11 mL, 22 mmol) in diethyl ether was added to a stirred solution of **5** (700 mg, 2.22 mmol) in dichloromethane (10 mL). The resulting solution was stirred for 16 h at room temperature (rt), and the solid formed was filtered and washed with anhydrous diethyl ether to yield **6** as a pale-yellow solid (537 mg, 96%). ^{1}H NMR (400 MHz, DMSO-d_6) δ 9.89 (s, 1H), 8.66 (s, 1H), 8.64–8.36 (m, 3H), 7.90–7.79 (m, 2H), 7.51–7.34 (m, 3H), 4.58 (d, $J = 6.1$ Hz, 2H), and 3.34 (q, $J = 5.8$ Hz, 2H). ^{13}C NMR (101 MHz, DMSO-d_6) δ 185.0, 152.6, 138.7, 132.1, 129.3,

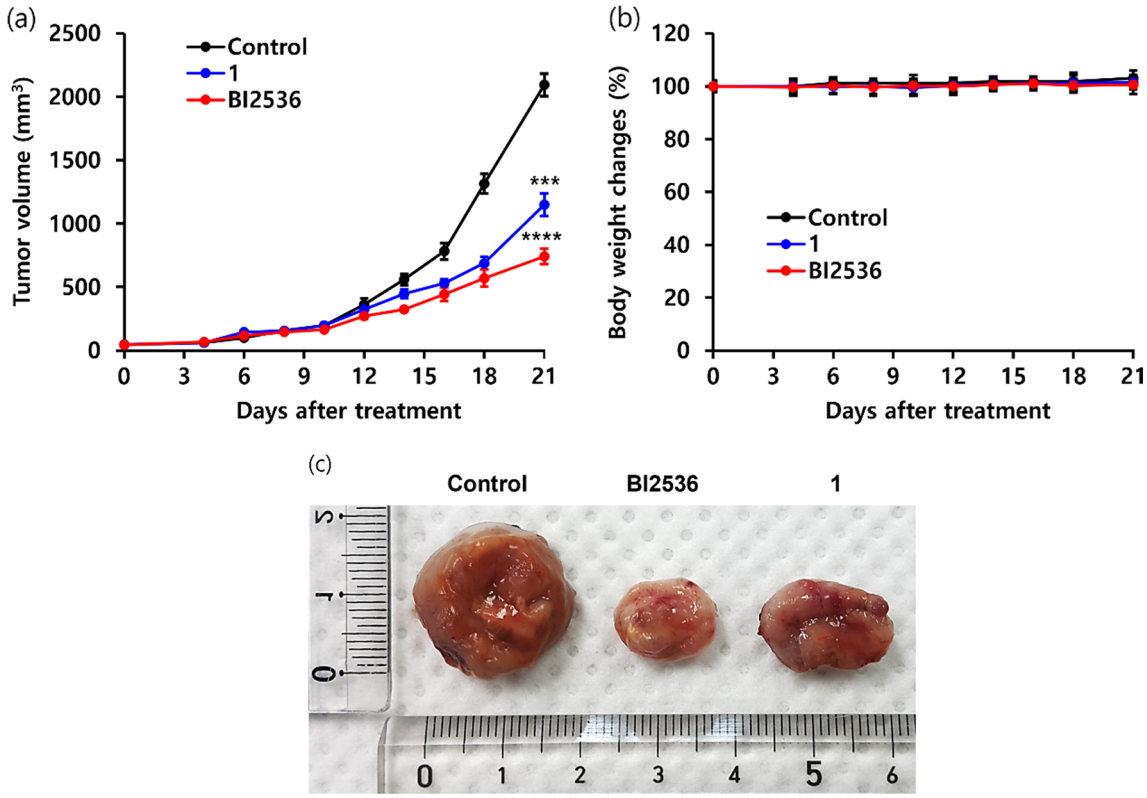

Fig. 7 Evaluation of in vivo anticancer effect of **1**. **a** The line graph represents the change in tumor volume caused by **1** and BI2536 (5 mg/kg of body weight). Tumor size changes are observed at 2- or 3-day intervals and values are expressed as mean ± standard deviation (n = 3). Tumor volume = length × width × height, mm^3. ***$p < 0.001$, ****$p < 0.0001$ **b** Body weight changes in the PBS, BI2536, and **1** treated groups up to 21 days are expressed in %. **c** Tumors picture of change in size

129.1, 128.9, 121.0, 49.5, and 38.7. MALDI-TOF m/z calculated for $C_{12}H_{13}N_3O$:215.10, found 215.44.

(9H-fluoren-9-yl)methyl4-((2-(3-phenyl-4-((2,4,6-trioxotetrahydropyrimidin-5(2H)-ylidene)methyl)-1H-pyrazol-1-yl) ethyl) carbamoyl)benzylcarbamate (8)

To a stirred solution of EDCI (607 mg, 3.18 mmol), HOBt (428 mg, 3.18 mmol) in DMF (10 mL), 4-(Fmoc-aminomethyl)benzoic acid (**7**) [1.1 g, 3.18 mmol], and DIEA (2.76 mL, 15.86 mmol) were added and stirred for 30 min. To the resultant solution, **6** (957 mg, 3.82 mmol) in DMF (5 mL) was added, and the mixture was stirred at rt for 18 h. The reaction mixture was treated with 5% $NaHCO_3$ solution (25 mL) and extracted with ethyl acetate (3 × 15 mL). The combined organic layer was washed with H_2O (3 × 20 mL) and brine, dried over Na_2SO_4, and evaporated under vacuum. To the crude product in methanol (15 mL), barbituric acid (0.269 g, 3.10 mmol) was added and refluxed for 16 h. The resulting yellow solid was filtered, washed with cold methanol (3 × 5 mL), and dried to yield the pure compound **8** as a yellow solid (1.08 g, 50%). ^{1}H NMR (400 MHz, DMSO-d_6) δ 11.24 (s, 1H), 11.21 (s, 1H), 9.35 (s, 1H), 8.65 (s, 1H), 8.16 (s, 1H), 7.89 (d, J = 5.6 Hz, 3H), 7.76 (d, J = 6.6 Hz, 2H), 7.71 (d, J = 6.4 Hz, 2H), 7.59–7.47 (m, 5H), 7.47–7.37 (m, 2H), 7.37–7.31 (m, 2H), 7.28 (d, J = 6.7 Hz, 2H), 4.58–4.45 (m, 2H), 4.44–4.32 (m, 2H), 4.30–4.16 (m, 3H), and 3.85–3.67 (m, 2H). ^{13}C NMR (101 MHz, DMSO-d_6) δ 167.0, 164.3, 163.2, 157.7, 156.9, 150.7, 144.9, 144.3, 143.6, 141.2, 139.1, 133.3, 131.7, 130.1, 129.5, 129.3, 128.1, 127.7, 127.5, 127.2, 125.6, 120.6, 113.9, 113.0, 65.8, 51.9, 47.3, and 44.0. MALDI-TOF m/z calculated for $C_{39}H_{32}N_6O_6$:680.23, found 703.2 $(M + Na)^+$.

4-(aminomethyl)-N-(2-(3-phenyl-4-((2,4,6-trioxotetrahydropyrimidin-5(2H)-ylidene)methyl)-1H-pyrazol-1-yl)ethyl) benzamide (1)

To the stirred solution of **8** (150 mg, 0.222 mmol) in DMF (1.4 mL), piperidine (0.6 mL) was added dropwise and stirred for 3 h. The solid formed was filtered, and the filtrate was treated with diethylether (30 mL). The precipitated solids were filtered and dried to yield **1** as a white solid (101 mg, 53%). ^{1}H NMR (500 MHz, DMSO-d_6) δ 8.52 (t, J = 4.8 Hz, 1H), 8.46 (s, 1H), 8.05 (s, 1H), 7.75 (d, J = 7.5 Hz, 2H), 7.66 (d, J = 7.5 Hz, 2H), 7.49 (t, J = 7.3 Hz, 2H), 7.42 (t, J = 7.2 Hz, 1H), 7.35 (d, J = 7.7 Hz,

2H), 4.68 (s, 2H), 4.42 (s, 2H), and 3.70 (s, 2H) [traces of diethyl ether were present]. ^{13}C NMR (101 MHz, DMSO-d_6) δ 166.9, 154.9, 151.4, 143.9, 133.2, 133.1, 132.1, 129.1, 128.9, 128.8, 128.5, 128.3, 127.7, 117.3, 64.6, and 51.7. MALDI-TOF m/z calculated for $C_{24}H_{23}N_6O_4$:458.17, found 459.13, 481.11 $(M+Na)^+$.

tert-butyl (4-((2-(4-formyl-3-phenyl-1H-pyrazol-1-yl)ethyl) carbamoyl)phenyl)-carbamate (10)

To a stirred solution of 4-(Boc-amino)benzoic acid (**9**) [52 mg, 0.20 mmol] in DMF (1 mL), EDCI (50 mg, 0.26 mmol), HOBt (40 mg, 0.30 mmol), and DIEA (0.183 mL, 1.00 mmol) were added for 10 min. Subsequently, **6** (50 mg, 0.20 mmol) was added, and the mixture was stirred for 16 h. The reaction mixture was treated with 5% $NaHCO_3$ solution (2.5 mL) and extracted with ethyl acetate (3×15 mL). The combined organic layer was washed with H_2O (3×10 mL), followed by brine solution, and evaporated under vacuum. The crude product was purified via silica gel column chromatography using ethyl acetate:hexane (8:2) mixture to obtain **10** as a yellow colored solid (0.179 g, 59%). ^{1}H NMR (400 MHz, DMSO-d_6) δ 9.86 (s, 1H), 9.62 (s, 1H), 8.53–8.49 (m, 2H), 7.82–7.80 (d, J=6.12 Hz, 2H), 7.74–7.71 (d, J=8.56 Hz, 2H), 7.52–7.49 (d, J=8.56 Hz, 2H), 7.46–7.44 (d, J=7.04 Hz, 2H), 4.40 (t, J=5.76 Hz, 2H), 3.72–3.70 (d, J=5.64 Hz, 2H), and 1.48 (s, 9H). MALDI-TOF m/z calculated for $C_{24}H_{26}N_6O_4$:434.496, found: 435.3127.

4-amino-N-(2-(3-phenyl-4-((2,4,6-trioxotetrahydropyrimidin-5(2H)-ylidene)methyl)-1H-pyrazol-1-yl)ethyl)benzamide (2)

To the reactant **10** (150 mg, 0.39 mmol) in methanol (5 mL), barbituric acid (0.043 g, 0.33 mmol) was added and refluxed for 16 h. The resulting solid was filtered through cold methanol (3×5 mL) and treated with TFA in DCM for 3 h at rt. The product was extracted with cold ether and further purified by HPLC to yield **2** as a yellow solid (100 mg, 53%). ^{1}H NMR (500 MHz, DMSO-d_6) δ 11.21–11.18 (d, J=13.6 Hz, 2H), 9.32 (s, 1H), 8.23 (t, J=5.55 Hz, 1H), 8.16 (s, 1H), 7.57–7.50 (m, 7H), 6.60–6.58 (d, J=8.5 Hz, 2H), 4.46 (t, J=5.95 Hz, 2H), and 3.68 (q, J=5.7 Hz, 4H). MALDI-TOF m/z calculated for $C_{23}H_{20}N_6O_4$:444.451, found: 445.2854.

4-(bromomethyl)-N-(2-(4-formyl-3-phenyl-1H-pyrazol-1-yl) ethyl) benzamide (12)

To a stirred solution of 4-(bromomethyl)benzoic acid (500 mg, 2.33 mmol) and $(COCl)_2$ (0.259 mL, 3.03 mmol) in DCM (20 mL) solvent, the catalytic amount of DMF was added dropwise and stirred for 3 h at rt. To the extract, **6** (642 mg, 2.58 mmol) was added and stirred for 4 h at rt. Then the product was obtained by column chromatography using ethyl acetate:hexane (65:35) mixture to obtain **12** as a colorless solid (702 mg, 75.3%). ^{1}H NMR (500 MHz, $CDCl_3$) δ 9.98 (s, 1H), 8.06 (s, 1H), 7.78–7.76 (m, 4H), 7.52–7.45 (m, 5H), 7.02 (s, 1H), 4.63 (s, 2H), 4.48 (t, J=5.35, 2H), and 4.01(q, J=5.6 Hz, 2H). MALDI-TOF m/z calculated for $C_{20}H_{18}BrN_3O_2$:412.287, found: 412.0136.

4-(bromomethyl)-N-(2-(3-phenyl-4-((2,4,6-trioxotetrahydropyrimidin-5(2H)-ylidene)methyl)-1H-pyrazol-1-yl)ethyl) benzamide (13)

To the stirred solution of **12** (400 mg, 0.97 mmol) in methanol (30 mL), barbituric acid (122 mg, 0.95 mmol) was added and refluxed for 16 h. The resulting crude extract was washed with cold methanol (4×20 mL) and recrystallized to yield the pure product **13** as a yellow solid (400 mg, 78.8%). ^{1}H NMR (400 MHz, DMSO-d_6) δ 11.22–11.19 (d, J=12.24 Hz, 2H), 9.35 (s, 1H), 8.70 (t, J=5.4 Hz, 1H), 8.15 (s, 1H), 7.82–7.80 (d, J=8.16 Hz, 2H), 7.54–7.48 (m, 7H), 4.80 (s, 2H), 4.51 (t, J=5.56 Hz, 2H), and 3.74 (q, J=5.36 Hz, 2H). MALDI-TOF m/z calculated for $C_{24}H_{20}BrN_5O_4$:522.359, found 522.0612.

4-(((2-aminoethyl)amino)methyl)-N-(2-(3-phenyl-4-((2,4,6-trioxotetrahydropyrimidin-5(2H)-ylidene) methyl)-1H-pyrazol-1-yl)ethyl)benzamide (3)

To the mixture of **13** (100 mg, 0.19 mmol) in methanol (10 mL), *N*-Boc-ethylenediamine (61 mg, 0.38 mmol) in DCM (10 mL) and DIEA (0.2 mL, 0.96 mmol) were added and allowed to stir for 36 h. The crude extract was dried under vacuum and treated with TFA (8 mL) in DCM (16 mL) for 18 h at rt. Subsequently, the solvent was removed under high vacuum and washed with cold ether to yield yellow solid, which was purified by HPLC and dried to obtain **3** as a yellow solid (27 mg, 33%). ^{1}H NMR (500 MHz, DMSO-d_6) δ 9.86 (s, 1H), 9.35 (s, 1H), 8.75 (s, 1H), 8.54 (s, 1H), 8.16–8.09 (m, 2H), 7.89–7.87 (d, J=8.3 Hz, 2H), 7.82–7.80 (m, 2H), 7.60–7.58 (d, J=8.3 Hz, 2H), 7.48–7.44 (m, 3H), 4.43 (t, J=5.75 Hz, 2H), 4.25 (s, 2H), 3.75 (q, J=5.7 Hz, 2H), and 3.29 (q, J=5.35 Hz, 4H). MALDI-TOF m/z calculated for $C_{26}H_{27}N_7O_4$:501.547, found 502.1445.

HeLa cancer cell viability assay by MTT

The HeLa cells were cultured in Dulbecco's modified Eagle's medium (DMEM) with 10% fetal bovine serum (FBS; Gibco, Invitrogen, USA) at 37 °C. Cells were seeded in 96-well plates (1×10^4 cells/mL per well in 100 μL medium). The cells were exposed to different concentrations of the derivatives (25, 50, 100, and 200 μM, 5% DMSO of final concentrion). After 24 h of culture, 10 μL of MTT assay (Enhanced Cell Viability Assay Kit, DoGenBio, Korea) was added to each well and left for

2–4 h. The MTT assay was performed using a microplate reader (Molecular Devices Corp, USA) at 470 nm absorbance.

Delocalization of Plk1 at the kinetochore by small molecule inhibitors

HeLa cells were cultured in DMEM supplemented with 10% (v/v) FBS in 24-well plates (2×10^4 cells/mL) at 37 °C in 5% CO_2. The cells were treated with DMSO, nocodazole (200 nM), BI2536 (200 nM), and their derivatives (200 μM) for 24 h. The medium in the wells was removed, and cells were fixed with 4% paraformaldehyde for 30 min. Fixed cells were permeabilized with 0.1% NP-40 in PBS for 10 min and washed with 1% bovine serum albumin in PBS three times. Lastly, cells were blocked with 5% bovine serum albumin in PBS for 30 min. Blocked cells were incubated with anti-Plk1 (mouse) and anti-Crest (human) antibodies for 2 h at rt, followed by incubation with Alexa Fluor 488 human anti-IgG and Texas Red mouse anti-IgG secondary antibodies at rt for 1 h. Fluorescence images were captured using an inverted Zeiss 710 confocal microscope (Carl Zeiss, Oberkochen, Germany). The signal intensity in each group was measured using the ZEN2010 program (Carl Zeiss, Oberkochen, Germany).

Cell cycle arrest by small molecule inhibitors via G2/M checkpoint

HeLa cells (4×10^5 cells, 6-well plates) were cultured along with BI2536 (200 nM) and the derivatives (200 μM) for 18 h based on the IC_{50} values of the inhibitors, and harvested by trypsinization. Harvested cells were fixed in 70% cold ethanol and stained with propidium iodide solution (Sigma Aldrich, USA) at 1 μg/mL concentration. Lastly, cells were treated with RNase (1 μg/mL, Thermo Scientific, USA) for 1 h at 37 °C. Flow cytometric analysis was performed using a fluorescence-activated cell sorter (Beckman Coulter, CytoFLEX, USA).

Effect of small molecule inhibitors on cell apoptosis in HeLa cancer cells

HeLa cells (1×10^4 cells) were seeded in 96-well plates along with BI2536 (200 nM), and the derivatives (200 μM) for 24 and 48 h. 100 μL of PBS (1 mL) mixed with 2.5 μL of fluorescence apoptosis kit (LIVE/DEAD™ Viability/Cytotoxicity Kit, Invitrogen™, USA) was added to each well in which cells were grown. After staining for 30 min at rt, the cells were observed under a fluorescence microscope (Nikon ECLIPSE TS100, Japan). The number of cells was calculated using the ImageJ software.

In vivo biological effect of small molecule inhibitors for cancer therapy

For in vivo tumor treatment study, 5×10^6 HeLa cells were subcutaneously injected into the right flank of 5-week-old BALB/c nude mice. When the tumor size reached 30 ± 10 mm^3, the mice were divided into groups of three mice each. Group 1 was treated with PBS only. Groups 2 and 3 were treated with BI2536 and **1**, respectively, via tail vein injection (5 mg/kg of body weight, 5% DMSO of final concentrion) at 2- or 3-day intervals for 21 days. To confirm that the tumor treatment effect of **1** was not caused by stress or external factors, weight change in the mice was observed. All animal experiments were conducted in accordance with the guidelines approved by the KBSI Committee (KBSI-AEC-1816).

Abbreviations

PPI	Protein–protein interactions
Plks	Polo-like kinases
PBD	Polo-box domain
5	Tert-butyl (2-(4-formyl-3-phenyl-1H-pyrazol-1-yl)ethyl)carbamate
4	Pyrazole aldehyde
6	Amine hydrochloride
rt	Room temperature
7	4-(Fmoc-aminomethyl)benzoic acid
9	4-(Boc-amino)benzoic acid
HeLa	Human cervical adenocarcinoma epithelial cell line
8	(9H-fluoren-9-yl)methyl4-((2-(3-phenyl-4-((2,4,6-trioxotetrahydropyrimidin-5(2H)-ylidene)methyl)-1H-pyrazol-1-yl)ethyl) carbamoyl) benzylcarbamate
1	4-(Aminomethyl)-*N*-(2-(3-phenyl-4-((2,4,6-trioxotetrahydropyrimidin-5(2*H*)-ylidene)methyl)-1*H*-pyrazol-1-yl)ethyl) benzamide
2	4-Amino-*N*-(2-(3-phenyl-4-((2,4,6-trioxotetrahydropyrimidin-5(2*H*)-ylidene)methyl)-1*H*-pyrazol-1-yl)ethyl)benzamide
12	4-(Bromomethyl)-*N*-(2-(4-formyl-3-phenyl-1*H*-pyrazol-1-yl)ethyl) benzamide
13	4-(Bromomethyl)-N-(2-(3-phenyl-4-((2,4,6-trioxotetrahydropyrimidin-5(2H)-ylidene)methyl)-1H-pyrazol-1-yl)ethyl)benzamide
3	4-(((2-Aminoethyl)amino)methyl)-N-(2-(3-phenyl-4-((2,4,6-trioxotetrahydropyrimidin-5(2H)-ylidene)methyl)-1H-pyrazol-1-yl)ethyl) benzamide
DMEM	Dulbecco's modified Eagle's medium
FBS	Fetal bovine serum

Acknowledgements
Not applicable.

Author contributions
YKL, GL, YSH and KD analyzed the data and wrote the manuscript. PG and MSY performed the experiments. MK, JKB and EKR conceptualized and designed the study. All authors read and approved the final manuscript.

Funding
This study was supported by a grant from the Korea Basic Science Institute (grant number C320000 & C330130).

Availability of data and materials
The datasets used and/or analyzed during the current study are available from the corresponding author upon reasonable request.

Declarations

Competing interests
The authors declare that they have no competing interests.

Received: 24 August 2023 Accepted: 1 November 2023
Published online: 27 November 2023

References

Archambault V, Glover DM. Polo-like kinases: conservation and divergence in their functions and regulation. Nat Rev Mol Cell Biol. 2009;10(4):265.
Cleary JM, Lima CMSR, Hurwitz HI, Montero AJ, Franklin C, Yang J, Holen K, et al. A phase I clinical trial of navitoclax, a targeted high-affinity Bcl-2 family inhibitor, in combination with gemcitabine in patients with solid tumors. Investigat New Drugs. 2014;32(5):937–45.
Corbi-Verge C, Kim PM. Motif mediated protein-protein interactions as drug targets. Cell Commun Signal. 2016;14(1):8.
Fode C, Motro B, Yousefi S, Heffernan M, Dennis JW. Sak, a murine protein-serine/threonine kinase that is related to the Drosophila polo kinase and involved in cell proliferation. Proc Natl Acad Sci U S A. 1994;91(14):6388–92. https://doi.org/10.1073/pnas.91.14.6388.
Gunasekaran P, Yim MS, Ahn M, Soung NK, Park JE, Kim J, Bang JK, et al. Development of a polo-like kinase-1 polo-box domain inhibitor as a tumor growth suppressor in mice models. J Med Chem. 2020;63(23):14905–20. https://doi.org/10.1021/acs.jmedchem.0c01451.
Karaman MW, Herrgard S, Treiber DK, Gallant P, Atteridge CE, Campbell BT, Edeen PT, et al. A quantitative analysis of kinase inhibitor selectivity. Nat Biotechnol. 2008;26(1):127.
Kothe M, Kohls D, Low S, Coli R, Rennie GR, Feru F, Ding YH, et al. Selectivity-determining residues in Plk1. Chem Biol Drug Des. 2007;70(6):540–6.
Lee KS, Burke TR Jr, Park J-E, Bang JK, Lee E. Recent advances and new strategies in targeting Plk1 for anticancer therapy. Trends Pharmacol Sci. 2015;36(12):858–77.
Lund-Andersen C, Patzke S, Nähse-Kumpf V, Syljuåsen RG. PLK1-inhibition can cause radiosensitization or radioresistance dependent on the treatment schedule. Radiotherapy Oncol. 2014;110(2):355–61.
Luo J, Emanuele MJ, Li D, Creighton CJ, Schlabach MR, Westbrook TF, Elledge SJ, et al. A genome-wide RNAi screen identifies multiple synthetic lethal interactions with the Ras oncogene. Cell. 2009;137(5):835–48.
Maire V, Némati F, Richardson M, Vincent-Salomon A, Tesson B, Rigaill G, Lang G, et al. Polo-like kinase 1: a potential therapeutic option in combination with conventional chemotherapy for the management of patients with triple-negative breast cancer. Cancer Res. 2013;73(2):813–23.
Park JE, Soung NK, Johmura Y, Kang YH, Liao C, Lee KH, Lee KS, et al. Polo-box domain: a versatile mediator of polo-like kinase function. Cell Mol Life Sci. 2010;67(12):1957–70.
Scharow A, Raab M, Saxena K, Sreeramulu S, Kudlinzki D, Gande S, Kuster B, et al. Optimized Plk1 PBD inhibitors based on poloxin induce mitotic arrest and apoptosis in tumor cells. ACS Chem Biol. 2015;10(11):2570–9.
Skwarczynska M, Ottmann C. Protein–protein interactions as drug targets. Fut Med Chem. 2015;7(16):2195–219.
Steegmaier M, Hoffmann M, Baum A, Lénárt P, Petronczki M, Krššák M, Quant J, et al. BI 2536, a potent and selective inhibitor of polo-like kinase 1, inhibits tumor growth in vivo. Curr Biol. 2007;17(4):316–22.
Strebhardt K. Multifaceted polo-like kinases: drug targets and antitargets for cancer therapy. Nat Rev Drug Discover. 2010;9(8):643.
Tse C, Shoemaker AR, Adickes J, Anderson MG, Chen J, Jin S, Nimmer P, et al. ABT-263: a potent and orally bioavailable Bcl-2 family inhibitor. Cancer Res. 2008;68(9):3421–8.
Vassilev LT, Vu BT, Graves B, Carvajal D, Podlaski F, Filipovic Z, Klein C, et al. In vivo activation of the p53 pathway by small-molecule antagonists of MDM2. Science. 2004;303(5659):844–8.
Weerdt BCVD, Medema RH. Polo-like kinases: a team in control of the division. Cell Cycle. 2006;5(8):853–64.
Yim H. Current clinical trials with polo-like kinase 1 inhibitors in solid tumors. Anticancer Drugs. 2013;24(10):999–1006.
Yun S-M, Moulaei T, Lim D, Bang JK, Park J-E, Shenoy SR, Soung NK, et al. Structural and functional analyses of minimal phosphopeptides targeting the polo-box domain of polo-like kinase 1. Nat Struct Mol Biol. 2009;16(8):876.

Publisher's Note